The membrane bound N-terminal domain of human adenosine diphosphate ribosylation factor-1 (ARF1)

Sarah M.A. Davies[a], Thad A. Harroun[a], Thomas Hauß[b], Sharon M. Kelly[c], Jeremy P. Bradshaw[a,*]

[a] *Department of Preclinical Veterinary Sciences, R.(D.)S.V.S., University of Edinburgh, Summerhall, Edinburgh EH9 1QH, UK*
[b] *Hahn-Meitner-Institut, Glienicker Straße 100, D-14109 Berlin, Germany*
[c] *Institute of Biomedical and Life Sciences, Joseph Black Building, University of Glasgow, Glasgow G12 8QQ, UK*

Received 5 February 2003; revised 23 April 2003; accepted 27 May 2003

First published online 7 July 2003

Edited by Irmgard Sinning

Abstract The small G protein adenosine diphosphate ribosylation factor-1 (ARF1) is activated by cell membrane binding of a self-folding N-terminal domain. We present a model of the human ARF1 N-terminal peptide in planar lipid bilayers, determined from neutron lamellar diffraction and circular dichroism data with molecular modelling. This amphipathic domain lies at a shallow membrane depth, ideal for regulation of the ARF1 bio-timer by rapid, reversible membrane binding. The helical region does not elongate upon membrane binding, leaving the connecting flexible linker region's length unchanged.

Key words: Adenosine diphosphate ribosylation factor; Phospholipid; Membrane; Neutron diffraction; Circular dichroism

1. Introduction

Adenosine diphosphate ribosylation factors (ARFs) form a family of small intracellular G proteins that become activated and function only on membrane surfaces. To accomplish this, they combine the characteristic GDP/GTP switch with a unique membrane/cytoplasm switch. Membrane binding is also crucial to the normal biological regulation of ARFs by their guanine exchange factor (GEF) proteins and GTPase activating proteins (GAPs).

A number of crystal structures have been published for the soluble, inactive forms of certain ARF proteins (e.g. [1,2]). Much less is known about the active, membrane bound structures of ARF, the details of which are crucial to our understanding of how these proteins function both as molecular switches and bio-timers in cells. The highly conserved N-terminal domain primarily controls the membrane binding of ARF1. It consists of an N-terminal myristoyl chain (Myr) linked to a self-folding peptide domain. Membrane binding by active ARF-GTP persists upon removal of Myr, but is completely abolished upon deletion of the N-terminal peptide [3]. Furthermore, a double mutation reducing the hydrophobicity of the N-terminal peptide accelerates dissociation of active ARF-GTP from membranes by 100-fold [4].

The membrane-binding domain is a helix assumed to lie approximately parallel to the membrane surface. The interaction of this domain of human ARF1 with membrane lipids is an early event in the multi-step ARF1 activation pathway [5]. Indeed, membrane binding is a necessary precursor to the large structural reorganisations of the core and switch regions of ARF1, which permit its activation by the appropriate GEFs (e.g. [6]). Membrane insertion of the N-terminal helix of ARF1 would facilitate a change to the open conformation that is required for ARF1 to bind its GEF [7].

The structural details of the membrane ARF1-GEF intermediates are not known. The helical region within the N-terminal domain of ARF1 may elongate upon membrane association [1]. Changes in the length of the helix, and thus the connecting flexible linker region, could affect the molecular reorganisation of the core and switch regions of ARF1 that occur along this pathway. Differences in the length of the flexible linker regions of ARF1 and ARF6 may contribute to the differences seen in the switch regions of these two ARF isoforms, which are thought to play an important physiological role [2]. To understand this role as a reversible membrane anchor, it is necessary to know the precise depth and orientation of the N-terminal peptide domain within a lipid bilayer. Here we present the directly observed location of three residues of ARF1's self-folding N-terminal peptide domain in planar phospholipid bilayers. From this we deduce the orientation, depth and probable structure of the peptide in the membrane.

2. Materials and methods

DOPC and DOPG were purchased from Avanti Polar Lipids (Birmingham, AL, USA). The 15 residue ARF1 peptide was synthesised and purified by Albachem (Edinburgh, UK) to the sequence in the Swiss Protein Data Bank. Four batches of the peptide were produced, one undeuterated and three deuterium-labelled at phenylalanines 5, 9 or 13. Each label involved replacing the 5 ring hydrogens with deuterium. 20 mg of DOPC and DOPG (70:30 mol%) and 3 mol% peptide were co-dissolved in chloroform/trifluoroethanol (TFE) and deposited by airbrush onto a silicon wafer. This produces highly aligned multi-bilayers in a standard manner. The wafers were placed under vacuum for 12 h to remove all traces of the solvent, before being rehydrated and annealed at 40°C in a humid atmosphere for at least 6 h. Samples were then mounted and aligned in sample cans 24 h before commencing data collection to allow full equilibration with the chosen sample conditions.

Neutron diffraction measurements were carried out on the V1 diffractometer at BENSC, Hahn-Meitner-Institut, Berlin, Germany. Samples were run at 25°C and the temperature was regulated by a

*Corresponding author. Fax: (44)-131-650 6139.
E-mail address: j.bradshaw@ed.ac.uk (J.P. Bradshaw).

0014-5793/03/$22.00 © 2003 Published by Elsevier Science B.V. on behalf of the Federation of European Biochemical Societies.
doi:10.1016/S0014-5793(03)00638-0

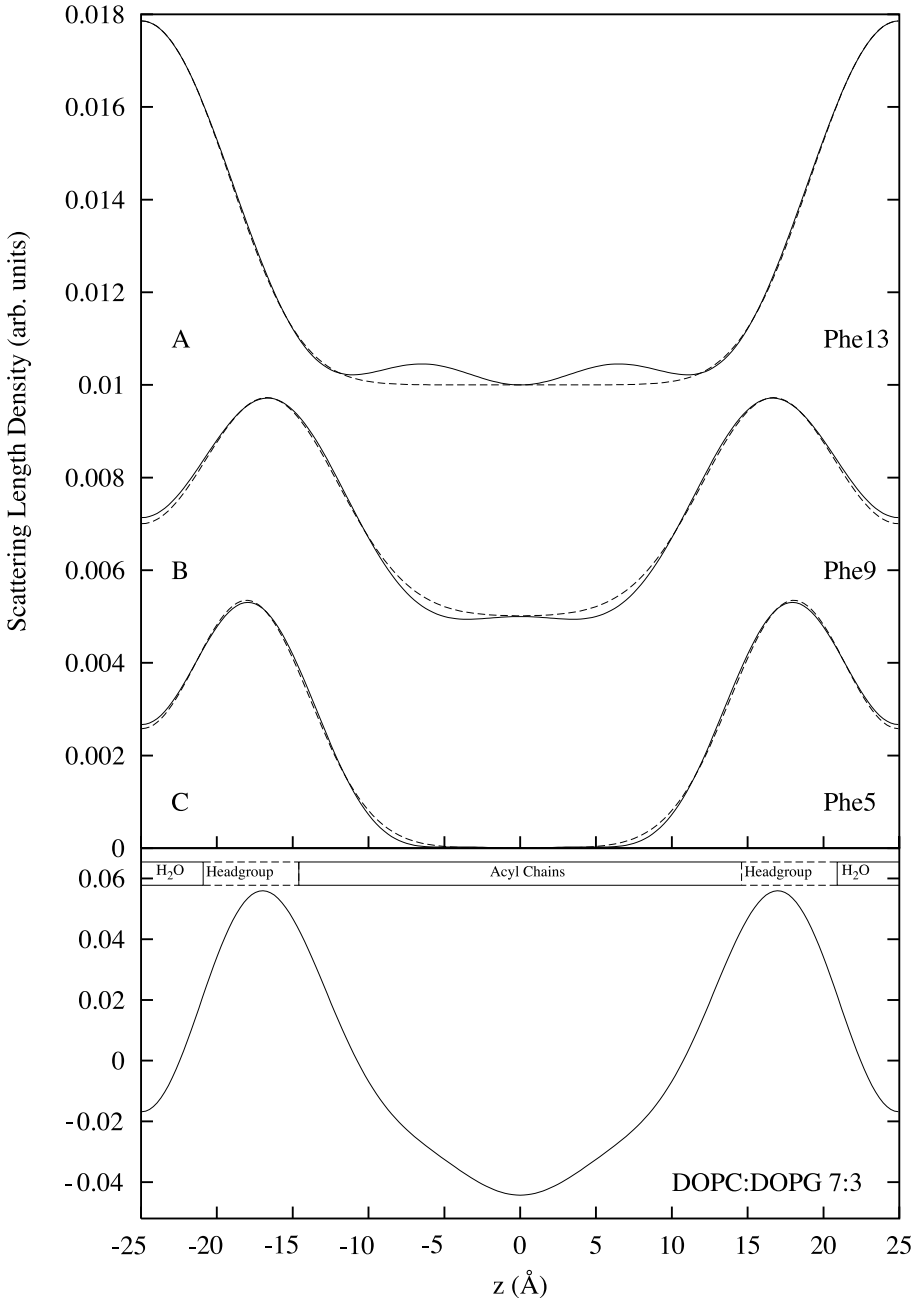

Fig. 1. Upper: (solid line) neutron scattering length density profiles of deuterium label in 3 mol% ARF1 N-terminal peptide in stacked multilayers of DOPC and DOPG, at 25°C and 92% relative humidity, 8% ^2H_2O; A: ($^2H_5$-Phe13); B: ($^2H_5$-Phe9); C: ($^2H_5$-Phe5). The data have been scaled using the relative absolute method [10–12]. (Dashed line) Gaussian models of the label residues. The position, width and size of Gaussian distributions (Table 2) were fitted, in reciprocal space, to observed differences in neutron structure factors. Lower: the total scattering length density of DOPC and DOPG in the molar ratio of 7:3. The water, lipid headgroup and acyl chain regions are shown for orientation. The unit cell length was 49.88 Å. NB. The vertical scale differs between the two panels.

circulating water bath. Small water baths containing saturated solutions of potassium chloride, potassium nitrate or potassium sulphate were placed inside the sample can to maintain the relative humidity of the sample environment at 85%, 92% or 97% respectively. Each sample was run at three ^2H_2O concentrations, 8%, 20% or 29%, and 50% ^2H_2O to provide additional phasing information. 8% ^2H_2O data were used for the difference calculations, since water of this isotopic composition has a net neutron scattering length density of zero. Two or three relative humidities were used for the 8% data; this improves data phasing and allows determination of accurate structure factors for the 8% data at the exact *d*-spacing as the 50% data [8]. The scanning protocol consisted of sequential θ (sample angle) scans around the predicted Bragg angle for each order.

Peak fitting and background subtraction were carried out using Peakfit (Jandel Scientific Software GmbH). Absorption and Lorentz corrections were applied and the intensities square-rooted to produce structure factor amplitudes. For each sample, the relative scaling of the data sets representing different ^2H_2O concentrations and the phases of each of their orders were determined by least-squares fitting to straight line functions. The whole procedure has been described previously [9]. The data were placed on a 'relative absolute' [10–12] scale using the known neutron scattering lengths of ^2H and ^1H. This method requires knowledge of the molar percentage of water in the samples, which was determined as previously described [13]. Four orders of diffraction were used in the fitting procedure, sufficient to give an accurate label position [14].

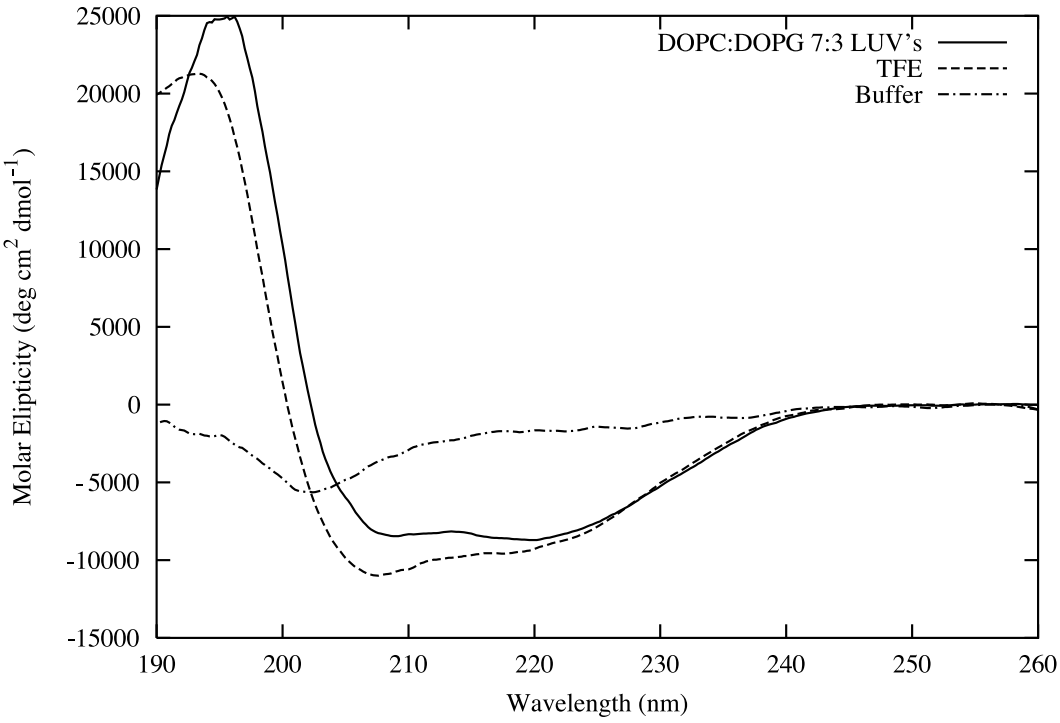

Fig. 2. CD spectra of ARF1 peptide in LUVs containing 30 mol% DOPG/70 mol% DOPC; 50% trifluoroethanol (TFE) and aqueous buffer. The spectra from peptide at two concentrations, 0.2125 mg/ml and 0.425 mg/ml, were similar.

For the circular dichroism (CD) measurements, large unilamellar vesicles (LUVs) containing 30 mol% DOPG/70 mol% DOPC were prepared from lipid films dried under nitrogen gas and then overnight under vacuum. The dried lipids were suspended in liposome buffer, 10 mM Tris, 0.1 mM EDTA, pH 7.4, vortexed vigorously and subjected to five freeze-thaw cycles by immersion in liquid nitrogen for 2 min and plunging into a 40°C water bath until thawed. Samples were then filtered 10 times through two stacked polycarbonate membranes, pore size 0.1 μm, using a high pressure extruder (Lipex Biomembranes Inc., Vancouver, Canada), as per the standard extrusion method of Hope et al. [15]. A stock solution of pre-lyophilised ARF1 peptide in liposome buffer was prepared. Peptide was added to the preformed LUVs to give a final peptide concentration of 0.2125 mg/ml or 0.425 mg/ml, and a lipid:peptide mole ratio of 16.5:1, 33:1 or 66:1. ARF1 peptide was also dissolved in liposome buffer and 50% TFE to give final peptide concentrations of 0.2125 mg/ml or 0.425 mg/ml.

CD spectra were recorded on a JASCO J-600 spectropolarimeter, using a sample cell of path length 0.02 cm. Each sample was scanned twice. The scan range was 195–260 nm, and the scan rate 10 nm/min. Background spectra were obtained for each sample, using 50% TFE and liposome buffer for the solvent studies, and LUVs at each lipid concentration for the ARF1 vesicle-binding studies. All sample spectra were thus background-corrected, as well as averaged and smoothed.

3. Results

3.1. Neutron diffraction

Using neutron diffraction and specific deuteration, we have determined the location and orientation of a 15 residue peptide from the N-terminus of human ARF1 (SWISSPROT #P32889) in an aligned bilayer. Neutron structure factors are shown in Table 1 and neutron scattering length density profiles, calculated from them, are shown in Fig. 1. The upper plots in Fig. 1 show the difference in scattering length density profiles between undeuterated ARF1 peptide in anionic lipid bilayers and three ARF1 peptides labelled at positions Phe5, Phe9, and Phe13, under the same sample conditions. The result is the distribution of deuterium labels across the bilayer normal. All three ^{2}H-Phe labels clearly show one discrete site

Table 1
Neutron structure factors of ARF1 peptide in bilayers of DOPC and DOPG (70:30 mol%), as used in the Fourier subtractions

	$F(1)$	$F(2)$	$F(3)$	$F(4)$
ARF1 peptide	-0.782 $\pm 8.8\times10^{-4}$	-0.606 $\pm 2.5\times10^{-4}$	0.473 $\pm 2.9\times10^{-4}$	-0.189 $\pm 4.1\times10^{-4}$
($^2H_5$-Phe5)-Arf1 peptide	-0.925 $\pm 5.0\times10^{-4}$	-0.676 $\pm 1.8\times10^{-4}$	0.550 $\pm 2.6\times10^{-4}$	-0.219 $\pm 3.0\times10^{-4}$
($^2H_5$-Phe9)-ARF1 peptide	-0.931 $\pm 5.2\times10^{-4}$	-0.707 $\pm 3.9\times10^{-4}$	0.555 $\pm 3.9\times10^{-4}$	-0.213 $\pm 3.1\times10^{-4}$
($^2H_5$-Phe13)-ARF1 peptide	-0.891 $\pm 8.2\times10^{-4}$	-0.578 $\pm 2.3\times10^{-4}$	0.470 $\pm 4.0\times10^{-4}$	-0.197 $\pm 4.2\times10^{-4}$
70% DOPC, 30% DOPG	-0.935 $\pm 1.4\times10^{-3}$	-0.541 $\pm 2.5\times10^{-4}$	0.523 $\pm 3.0\times10^{-4}$	-0.327 $\pm 3.2\times10^{-4}$

Structure factors for bilayers of DOPC and DOPG (70:30 mol%) are also shown, for comparison. Data were collected at 25°C, 85%, 92% or 97% relative humidity and 8% ^2H_2O [12].

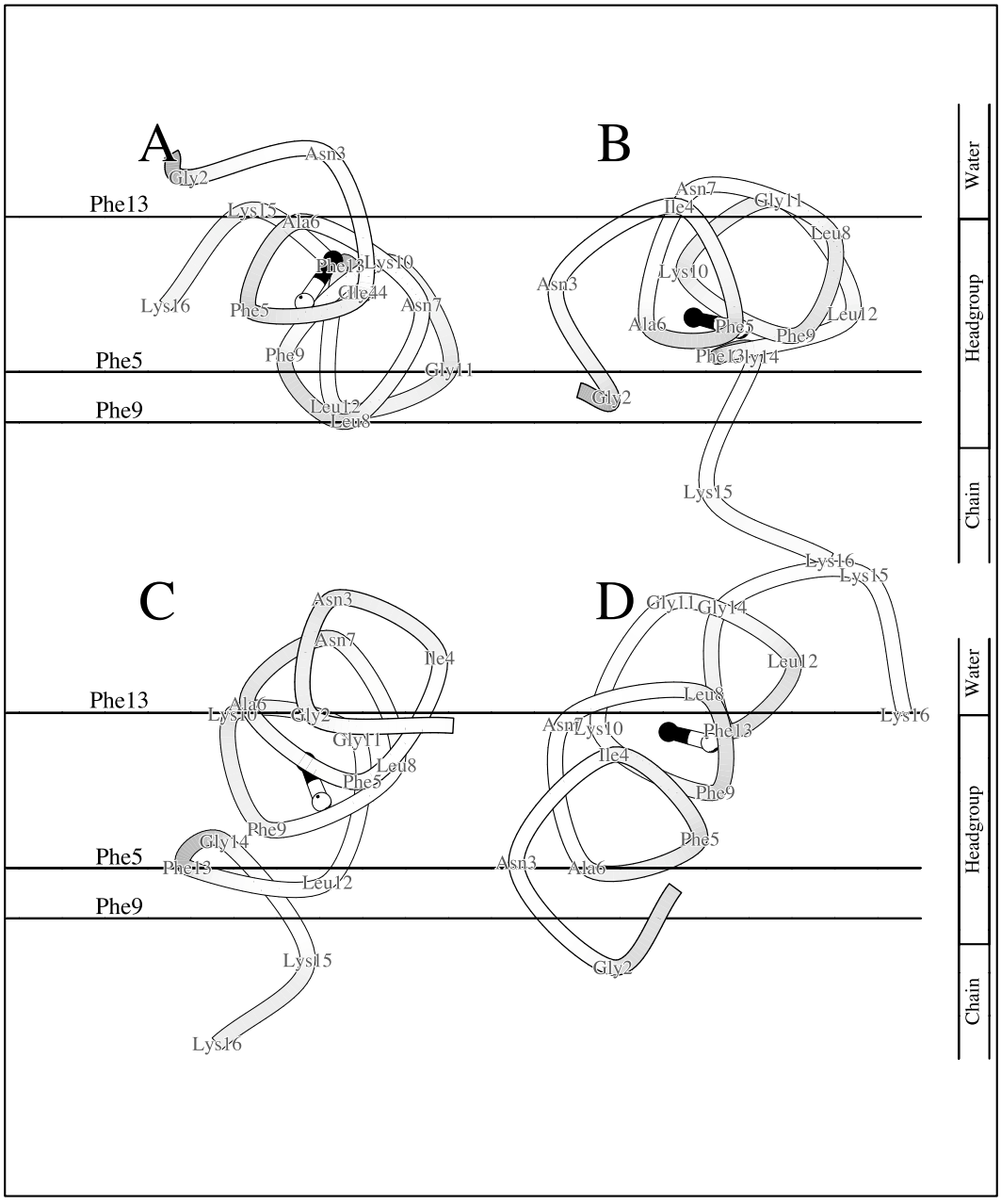

Fig. 3. The peptide models drawn as ribbon diagrams, which view the peptides along the surface of the bilayer. The diagram shows the relative depth in the bilayer of the peptide's α-carbons. As in Fig. 1, the water, lipid headgroup and acyl chain regions are shown for orientation. The solid, horizontal lines indicate the measured depths of the labels. Models A and B are the two possible orientations of the peptide taken directly from the crystal structure of the full-length protein [1]. Models C and D were calculated by confining the phi–psi angles of the crystal-derived model to an α-helix, and then orienting to the label data. For a detailed discussion of the merits of each model, please refer to the text.

on each side of the bilayer, indicating that the ARF1 peptide adopts one orientation, or location, which is within the interfacial region of the membrane. To ensure reliability, data on the ARF peptide specifically deuterated at position 13 were obtained from two independent experiments.

In order to calculate the difference profiles accurately, it is first necessary to scale the various data sets to each other. For a pure lipid structure, it is possible to use the known neutron scattering lengths of the phospholipid and its component parts [10–12]. This is not always possible when a peptide is present, because the details of the structure are not known. In these circumstances, it is normal to use the known neutron scattering length of deuterium, introduced into the system in exchange for hydrogens. In this study, seven independent deuterium exchanges were carried out, namely the three deuterated amino acids and ^2H_2O–H_2O exchange with each of the four different peptides (for method see [16]). The fact that consistent scale factors were calculated from all seven increases our confidence in the data. It also means that, by definition, the size (area under the peaks) of the label distributions shown in Fig. 1A–C is exactly right for the number of deuterons in each of the samples measured.

The neutron scattering length density profiles of bilayers with peptide can be difficult to understand and of limited interpretational value. The observed differences between these profiles and that of pure phospholipid are small. It is impos-

sible to deconstruct the changes caused by scattering from the peptide itself from the changes in scattering caused by the redistribution of the phospholipids necessary to accommodate the peptide. The situation is made more complex by the artefacts introduced by termination error. The difference method, as used to produce the profiles shown in Fig. 1A–C, simplifies the picture by removing the contributions of water, phospholipid and undeuterated parts of the peptide. The resulting profile can be fitted to a single Gaussian distribution. If the fitting process is carried out in reciprocal space, as in this case, the effects of termination error are also avoided.

3.2. CD

It is expected that the N-terminal peptide domain of ARF1 will self-fold into its active conformation only in a membrane environment. Fig. 2 shows the CD results, which support this prediction. In aqueous buffer, the peptide's structure was random coil. The secondary structure promoting solvent trifluoroethanol induces some helicity, but the highest overall amount of secondary structure was found in LUVs containing 30 mol% DOPG/70 mol% DOPC (Fig. 2). At lipid/peptide ratios where the entire ARF1 domain was membrane bound, which include that used for the neutron diffraction work, estimates of the amount of helix present in the peptide ranged from 28% to 36% [17,18]. From the crystal structure, this domain is only partially α-helix, the rest being non-specific helix and coil that connects to the linker region. There is no indication of a large increase in helical conformation on membrane binding.

3.3. Modelling

The difference profile of neutron scattering length density gives the time-averaged, Gaussian distribution of the centre of mass for the five deuterons around the ring of each labelled phenylalanine. Our goal was to find the orientation of the ARF1 peptide such that the depth of each phenylalanine ring in the model coincided with the data. We used the same method previously to determine the position of a fusion peptide within a lipid membrane [19]. As explained in that paper, four independent labels are required to orient a protein unambiguously. In the current case, with only three labels, we are left with two models that must be evaluated using other criteria.

As a starting point for modelling our data, we used the coordinates of the N-terminal domain present in the crystal structure of human ARF1-GDP [1]. Fig. 3A,B representates schematically the two possible orientations from the crystal structure model, as viewed along the surface of the membrane. The horizontal lines indicate the depth in the bilayer of the labels, where the vertical scale shows the bilayer profile. Both orientations indicate ARF1 lies almost exactly parallel to the bilayer surface, at an angle of less than 5° from the membrane surface, as determined by fitting a straight line to the backbone. However, orientation B is highly thermodynamically unfavourable, because the predicted hydrophobic face of model B is partially exposed to the water side of the lipid–water interface. The charged lysines 15 and 16 are placed far too deeply in the hydrophobic core of the membrane. Furthermore, isoleucine 4 is unexpectedly found to be exposed to the aqueous environment. Fig. 4 shows how model A lies within the lipid headgroups. The lower surface in Fig. 4 represents the centre of the bilayer, and the upper surface the hydrophobic–hydrophilic interface.

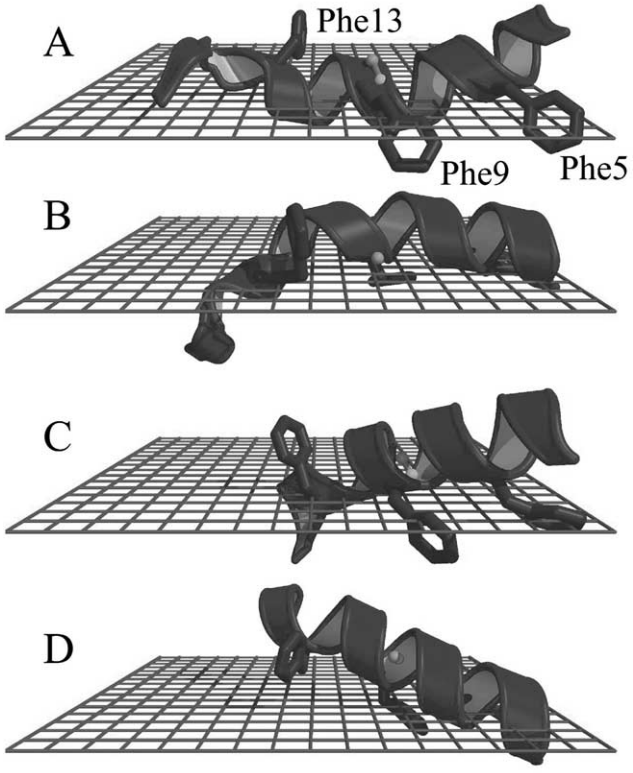

Fig. 4. The molecular structure of ARF1 peptide oriented in one half of a bilayer. The vertical line is the *z*-axis scale parallel to the membrane normal. The lower lattice represents the centre of the bilayer, and the upper lattice at the approximate value of 16 Å suggests the hydrophobic/hydrophilic interface. The peptide helix is represented as a coiled ribbon, while the deuterated residues Phe5, Phe9, and Phe13 are represented as stick models. This orientation is model A in Fig. 2, and is the best fit to the experimental data. The figure was prepared with Molscript [22] and Raster3D [23].

To test the idea that the N-terminal helix extends past residue 13 upon binding to the membrane, we used the Sybyl

Table 2
Gaussian models of deuterium label distribution of 3.0% (mol) ($^2H_5$-Phe5)-, ($^2H_5$-Phe9)- and ($^2H_5$-Phe13)-ARF1 peptide in bilayers of DOPC and DOPG (70:30 mol%)

	Phe5	Phe9	Phe13
Amplitude	$0.0551 \pm 2.4 \times 10^{-4}$	$0.0555 \pm 3.9 \times 10^{-4}$	$0.0520 \pm 3.7 \times 10^{-4}$
Position[a]	$17.99 \pm 1.9 \times 10^{-2}$ Å	$16.68 \pm 3.6 \times 10^{-2}$ Å	$22.06 \pm 5.6 \times 10^{-2}$ Å
Width[b]	$5.83 \pm 3.0 \times 10^{-2}$ Å	$6.64 \pm 4.3 \times 10^{-2}$ Å	$5.88 \pm 7.9 \times 10^{-2}$ Å
Chi-squared	2.1×10^{-5}	7.2×10^{-5}	7.0×10^{-6}

The position, width and size of Gaussian distributions were fitted, in reciprocal space, to difference neutron structure factors. Four orders of diffraction were used in the fitting procedure.
[a]The position of each label site is expressed as distance from the centre of the bilayer.
[b]The width is the full width at 1/e height.

modelling software (Tripos) and constrained the phi, psi angles of the crystal structure model to those of an α-helix. We then performed 1000 steps of energy minimisation to remove forbidden contacts that might have been created. Fig. 3C,D shows that this new model is substantially tilted out of the membrane plane, to an angle of about 20°. This orientation lifts leucines 8 and 12 unacceptably out of the bilayer (model C), or pushes lysines 15 and 16 even further into the bilayer (model D). Furthermore, an ab initio α-helix constructed from the sequence cannot be oriented to fit the data at all. When constrained to a helix, the Phe13 moves closer to the same face of the peptide as Phe5 and Phe9, and therefore cannot bridge the large measured gap between these residues. Combining these findings with the CD data, which indicates that the membrane bound peptide is not completely helical, we believe that the helix must be terminated before residue 13 of the ARF1 N-terminal domain, and does not extend upon membrane binding.

Each panel of Figs. 3 and 4 also shows the corresponding hydrophobic vector, defined as the vector between the hydrophobic and hydrophilic barycentres [20]. The barycentres were calculated by the method and transfer energies of Brasseur [20].

4. Discussion

Reversible membrane binding regulates many proteins and enzymes involved in cell signalling; for a recent review see [21]. Little is known about how membrane binding regulates the function of these amphitropic proteins; detailed structural information is a prerequisite to understanding this process. Our neutron diffraction studies provide unique direct information on the nature of the interaction of the ARF1 N-terminal peptide with flat lipid membranes that resemble biological membranes in their packing properties. From these results, it seems likely that the ARF1 self-folding N-terminal domain changes its internal structure very little during the membrane–cytoplasm cycle of the ARF protein. If we model the structure of the N-terminus as in the soluble, inactive ARF1-GDP protein and fit it to our label positions for ARF1 when membrane bound, the peptide lies almost exactly parallel to the membrane surface. This nicely agrees with thermodynamic predictions. Conversely, extending the helix such that it includes the last label in our peptide, Phe13, cannot be supported by the data. Thus we believe that the helix of ARF1 does not extend upon membrane binding. This also leaves the proximal portion of the ensuing linker region unchanged in length. This may be important to allow the remainder of the ARF protein sufficient structural flexibility to interact simultaneously with the cell membrane, a GEF protein, GDP/GTP and a GAP protein – a remarkable feat indeed!

Acknowledgements: We thank Thomas Gutberlet and Silvia Dante for expert technical assistance with V1 at the HMI, Nicholas Price and the BBSRC for access to the Scottish Circular Dichroism centre. Support for use of the BENSC facilities at the HMI was provided by the European Commission, under the Human Potential Programme's Access to Research Infrastructures action. S.M.A.D. was a Wellcome Trust International Fellow.

References

[1] Amor, J.C., Harrison, D.H., Kahn, R.A. and Ringe, D. (1994) Nature 372, 704–708.
[2] Ménétrey, J., Macia, E., Pasqualato, S., Franco, M. and Cherfils, J. (2000) Nat. Struct. Biol. 7, 466–469.
[3] Franco, M., Chardin, P., Chabre, M. and Paris, S. (1993) J. Biol. Chem. 268, 24531–24534.
[4] Antonny, B., Béraud-Dufour, S., Chardin, P. and Chabre, M. (1997) Biochemistry 36, 4675–4684.
[5] Béraud-Dufour, S., Paris, S., Chabre, M. and Antonny, A. (1999) J. Biol. Chem. 274, 37629–37636.
[6] Goldberg, J. (1998) Cell 95, 237–248.
[7] Roth, M.G. (1999) Trends Cell Biol. 9, 174–179.
[8] Darkes, M.J.M. and Bradshaw, J.P. (2000) Acta Crystallogr. D 56, 48–54.
[9] Duff, K.C., Gilchrist, P.J., Saxena, A.M. and Bradshaw, J.P. (1994) Virology 202, 287–293.
[10] Wiener, M.C., King, G.I. and White, S.H. (1991) Biophys. J. 60, 568–576.
[11] Wiener, M.C. and White, S.H. (1991) Biophys. J. 59, 162–185.
[12] Jacobs, R.E. and White, S.H. (1989) Biochemistry 28, 3421–3437.
[13] Bradshaw, J.P., Davies, S.M.A. and Hauss, T. (1998) Biophys. J. 75, 889–895.
[14] Gordeliy, V.I. and Chernov, N.I. (1997) Acta Crystallogr. D 53, 377–384.
[15] Mayer, L.D., Hope, M.J. and Cullis, P.R. (1986) Biochim. Biophys. Acta 858, 161–168.
[16] Bradshaw, J.P., Davies, S.M.A. and Hauß, T. (1998) Biophys. J. 75, 889–895.
[17] Sreerama, N. and Woody, R.W. (1993) Anal. Biochem. 209, 32–44.
[18] Bohm, G., Muhr, R. and Jaenicke, R. (1992) Protein Eng. 3, 191–195.
[19] Bradshaw, J.P., Darkes, M.J.M., Harroun, T.A., Katsaras, J. and Epand, R.M. (2000) Biochemistry 39, 6581–6585.
[20] Brasseur, R. (2000) Mol. Membr. Biol. 17, 31–40.
[21] Johnson, J.E. and Cornell, R.B. (1999) Mol. Membr. Biol. 16, 217–235.
[22] Kraulis, P.J. (1991) Appl. Crystallogr. 24, 946–950.
[23] Merritt, E.A. and Bacon, D.J. (1997) Methods Enzymol. 277, 505–524.